

Insight into the mechanism of persulfate activated by bone char: unraveling the role of functional structure of biochar

Xuerong Zhou ^{a,1}, Zhuotong Zeng ^{b,1}, Guangming Zeng ^{a,*}, Cui Lai ^{a,*}, Rong Xiao ^{b,*},
Shiyu Liu ^a, Danlian Huang ^a, Lei Qin ^a, Xigui Liu ^a, Bisheng Li ^a, Huan Yi ^a, Yukui Fu ^a,
Ling Li ^a, Mingming Zhang ^a, Zhihong Wang ^a.

^a College of Environmental Science and Engineering, Hunan University and Key Laboratory of Environmental Biology and Pollution Control, Hunan University, Ministry of Education, Changsha 410082, PR China,

^b Department of Dermatology, Second Xiangya Hospital, Central South University, Changsha 410011, P R China.

* Corresponding author at: College of Environmental Science and Engineering, Hunan University, Changsha, Hunan 410082, China. Tel: +86-731-88822754; fax: +86-731-88823701. E-mail address: zgming@hnu.edu.cn (G.M. Zeng) , laicui@hnu.edu.cn (C.Lai) and xiaorong65@csu.edu.cn (R. Xiao).

¹ These authors contribute equally to this article.

Abstract

Recently, biochar was frequently applied in catalysis field, and it has been regarded as an efficient carbon-rich material to degrade organic pollutants in water. Various functional structures of biochar (such as pore structure, oxygen-containing groups and defects) have been reported to be valid in catalysis. Whereas the complexity of biochar structure and composition hinders the further exploration of specific functions of biochar. To address this problem, selective inactivation experiment was first involved to investigate the role of oxygen-containing groups in catalysis. In this study, swine bone derived biochar (BBC) was adopted as catalyst in persulfate (PS) activation system to degrade acetaminophen (ACT). Both non-radical and radical pathway worked in BBC/PS system. ACT could be completely degraded in 60 min, and the removal rate could reach 0.3111 min^{-1} . The results showed that the ketone groups on the BBC were the primary active sites of PS/BBC system and it played a major role in non-radical pathway (electron transfer pathway), and it might act as the active sites to produce $\cdot\text{OH}$ in BBC/PS system. Besides, the $-\text{COOH}$ and $-\text{OH}$ on BBC might be beneficial to radical pathway, which can help to generate $\cdot\text{OH}$ and $\text{SO}_4^{\cdot-}$. Interestingly, residual hydroxyapatite and defects in BBC might be able to stimulate PS to produce $\text{O}_2^{\cdot-}$ and $^1\text{O}_2$. With the development of increasingly precise biochar synthesis techniques, these verdicts give evidence to further oriented synthesis of biochar.

Keywords: Persulfate; Bone char; Functional structures; Catalysis; Acetaminophen

1. Introduction

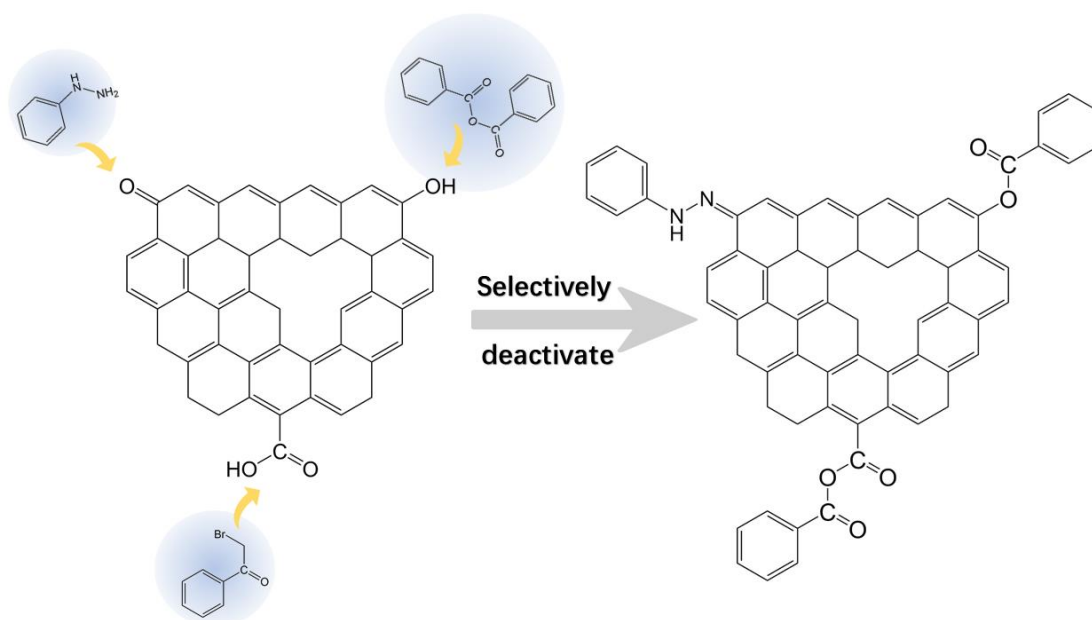
Advanced oxidation processes (AOPs) are broadly applied in water treatment process, since its strong oxidation capacity can completely mineralize the refractory contaminants in aqueous media [1-4], including methods such as photocatalysis [5-14], electrocatalysis [15], Fenton oxidation [16] and ozonation [17]. Considering persulfate (PS) is more economical (\$0.74/kg versus \$1.5/kg of hydrogen peroxide) and more convenient for storage and transportation than that of hydrogen peroxide, the PS activation system is gradually developed as an important branch of AOPs in these years [18]. **The PS activation system primarily works through radical and non-radical pathway, $\text{SO}_4^{\cdot-}$ is distinct among various worked radical species.** Furthermore, it possesses a relatively high redox potential and long lifetime, which is helpful for the complete mineralization of pollutants in water [19]. Initially, metal ions and metal oxides were used to efficiently catalyze PS. Furthermore, Wang and his group proved that carbonaceous materials could also act as catalysts in PS activation system [20, 21]. Then, biochar as a common carbonaceous material got into the sight of researchers.

Biochar is a simple-design and low-cost rich-carbon solid material, which is produced by the pyrolysis of biomass. There is a rising consensus that biochar is a deliberate manner in soil remediation [22] and carbon sequestration fields [23]. Recently, biochar has been used as a new species of carbonaceous catalyst in AOPs field [24]. Empirically, researchers have reported that functional structures of biochar (such as defects, oxygen-containing groups, persistent free radicals and pore structure) served as the active sites in catalysis field. Yu and his group reported that ketone structure inside

the biochar was the active sites for the degradation of bisphenol A [25]. Zhou and co-workers unveiled the role of persistent free radicals in organic contaminant degradation [26]. Besides, oxygen-containing groups were more frequently reported to play an important role in PS activation system [27, 28]. It is meaningful to understand the underlying mechanism of the functional structures, because the functional structures determine the active species in AOPs. On account of the complex composition and structure of biochar, the specific effect of different functional structures is hard to be investigated clearly. Overall, taken the effect of functional structures on mechanism and the increasingly precise synthesis processes of biochar into consideration, the oriented synthesis of biochar might be achieved in further application. Thus, it is urgent to develop a method to research the role of functional structures of biochar in AOPs system.

In general, the exploration of the mechanism is achieved by analyzing the change of material structure before and after the reaction [29, 30]. However, the recovery processes of materials might have certain impact on the results of instrumental analysis, which may ultimately affect the analysis of mechanism. With the development of chemical theory and technology, researchers have proposed a method to identify the oxygen-containing groups on carbonaceous materials by chemical titration. To be specific, this method aimed at selectively deactivating oxygen-containing groups by organic agent [31, 32]. It sheds light on the conclusion that the 2-Bromo-1-phenylethanone (BrPE), phenylhydrazine (PH), benzoic anhydride (BA) and could deactivate carboxyl (-COOH), ketone (C=O) and hydroxyl (-OH) on carbon materials respectively and have no effect on other feature structure (Scheme 1). Taken advantage of the idea of controlling variables, it might be a

feasible way to further explore the influence of oxygen-containing groups in catalysis. Guo and co-workers applied the chemical titration mentioned above to investigate the non-radical pathway of PS activation system [33].



Scheme 1 The chemical deactivation processes for ketonic ketone, hydroxy and carboxylic groups on BBC.

Our previous study had introduced bone derived char (BBC) in PS activation system to degrade 2,4-dichlorophenol (2,4-DCP) [29]. The BBC after reaction was collected for further analysis, and it manifested that oxygen-containing groups served as the active sites in BBC/PS system. Radical and non-radical pathway had been proved working in BBC/PS system, and both of them relied on the adsorption of BBC. Since the adsorption process might work through chemical and physical adsorption, it was difficult to ensure that the surface of BBC is not affect by adsorbate. So, the investigation of the mechanism by existing method remains to be further discussed. Besides, previous method could not study the concrete role of oxygen-containing groups. Accordingly, the introduction of

selective deactivated experiment is imperative.

As a typical kind of pharmaceutical and personal care products (PPCPs), acetaminophen (ACT) is the main ingredient in analgesic [34, 35]. ACT is frequently detected in municipal wastewater, because it is one of most consumed PPCPs in many countries [36]. The long-term exposure would not only take adverse effect to ecological systems, but also disrupt the human endocrine system and even result in cancer. Comparing to 2,4-DCP, the benzene ring in ACT possesses different substituent groups. Specifically, the halogens in the benzene ring denotes as the electron-withdrawing groups, which would suppress the electron cloud density of benzene ring. However, the acetamido group on ACT is electron-donating group. In order to understand effect of different type of substituents on BBC/PS system, this study chose ACT as the aim contaminant.

In order to confirm the variation of mechanism brought by the structure changes, liner sweep voltammetry (LSV) and **active species** capturing experiment were conducted by all BBC derivatives. Furthermore, the effect of functional structures of catalytic capacity was further explored by physical and chemical characterization, including electron spin resonance analysis (ESR), X-Ray diffraction (XRD), Raman spectra, X-ray photoelectron spectroscopy (XPS), etc.

2. Materials and methods

2.1 The preparation of biochar and materials

The swine bone derived biochar was synthesized by the pyrolysis of de-fatted spareribs. **The de-fatted process was accomplished by cooking.** Collected cooked bones were first carbonized by tuber furnace in the N₂ atmosphere at 450 °C. Pre-carbonized

particles were further carbonized at 900 °C (hold for 2 h). The 150 mL of 6 M HNO₃ was used to further process the products. After rinsing to neutral and drying out, the obtained materials were labelled as BBC. Furthermore, the materials not treated with acid were labelled as BBC-WA. BBC-1300 was obtained from further pyrolysis of BBC in tube furnace (1300 °C, 2 h).

2-Bromo-1-phenylethanone (BrPE, 99%), phenylhydrazine (PH, 99%), and benzoic anhydride (BA, 99%) were used to selectively deactivate the functional groups on BBC, for they could selectively react with carboxylic groups (-COOH), ketone (C=O), and hydroxyl (-OH) on carbon materials, respectively (detailed modification process was presented in supplementary information). Modified materials were labelled as BBC-BrPE, BBC-PH and BBC-BA, respectively. All chemicals were bought from sinopharm chemical reagent Co., Ltd., which were of reagent grade and used as received.

2.2 Catalytic experimental process

All batches were taken in the same beaker at room temperature. In order to evenly distribute the materials, magnetic stirring apparatus was applied. 1-hour-adsorption experiment was conducted to differentiate the effect of adsorption and catalysis. Firstly, 100 mg/L prepared BBC was dispersed into the solution (ACT, 20 mg/L). After 1 h adsorption, the PS of the same weight (1 g/L) was added into the solution, and the catalytic process began. After filtering by 0.22 µm nylon filter, the samples were collected at each predetermined interval. Na₂SO₄, NaCl, and NaNO₃ were used as the additive of SO₄²⁻, Cl⁻ and NO₃⁻ to assess the effect of common inorganic anions. After each run, BBC was treated with 0.1 M HNO₃, and then rinsed by ethanol and ultrapure water to

neutral. The stability tests were accomplished by drying these collected BBC. Ethanol (EtOH), tert-butyl-alcohol (TBA), benzoquinone (BQ), NaN₃, and K₂CrO₄ were chosen as the quenching agent in this experiment, for they could selectively scavenge different species active species and electron effectively.

2.3 Characterization of catalyst

XPS (ESCALAB 250Xi spectrometer, K-Alpha), XRD and Raman spectra were taken to detect the structure and constituent of the prepared materials. Raman spectra was conducted on LabRAM HR800 with 325 nm He-Cd laser, and XRD (Rigaku Dmax 2500, Japan) was in range from 10 ° to 80 °. Except for XPS, the surface functional groups of samples were also analyzed by FT-IR (IRTracer-100, Japan). The Brunauer-Emmett-Teller (BET) gas adsorption isotherm was taken on Quantachrome Autosorb AS-1 with N₂ to measure the specific surface area.

2.4 Analysis

The variation of ACT was measured by high performance liquid chromatography (Agilent 1200, C18 column (5.0 μm, 4.6 mm x 250 mm)). The mobile phase was combined by methanol and water (30:70, v/v), while the flow rate was 1 min/L (the column worked at 40 °C). The UV detector set at 243 nm. CHI760E electrochemical workstation served as the instrument to measure LSV. Bruker ER200-SRC was applied to measure ESR, which was used for verifying the generation of different active species. 5,5-dimethyl-1-pyrroline N-oxide (DMPO) and 2,2,6,6-tetramethylpiperidine (TEMP) were chosen as a trapping agent to identify active species. The SO₄^{•-}, ·OH were detected in deionized water, while O₂^{•-} was detected in methanol circumstance.

3. Results and discussion

3.1 Catalytic performance of BBC for ACT degradation

As mentioned above, previous study has proved that the BBC/PS system could degrade 2,4-DCP effectively [29]. Ren and co-workers reported that substituents of phenols did influence the degradation effect of PS activation system [37]. In order to understand effect of different types of substituents on BBC/PS system, this study chose ACT as the aim contaminant. Pre-experiment result showed that BBC/PS system could conspicuously accelerate the process of ACT degradation (Fig S1).

For further investigating the kinetics of this reaction, pseudo-first-order kinetics based on Langmuir-Hinshelwood model was fitted. The high regression coefficients manifest the reaction conforms to first order kinetics equation. k_{obs} is the label of the pseudo-first-order rate constant, and it is obtained by Eq. (1). The calculation illuminated that the k_{obs} of this system reaches 0.3111 min^{-1} . Comparing to other degradation methods, BBC/PS system possesses a remarkable degradation capacity for ACT (Table S1), which means BBC/PS system might be a proven pathway to manage micropollutant.

$$\ln(C/C_0) = -k_{obs}t \quad (1)$$

ESR have confirmed the existence of active species in BBC/PS system, while DMPO and TEMP were chosen as the trapping agents. As presented in Fig. 1, $\text{SO}_4^{\cdot-}$, $\cdot\text{OH}$, $\text{O}_2^{\cdot-}$ and $^1\text{O}_2$ all emerged in BBC/PS system, and the concentration of all active species had a tendency to increase with time.

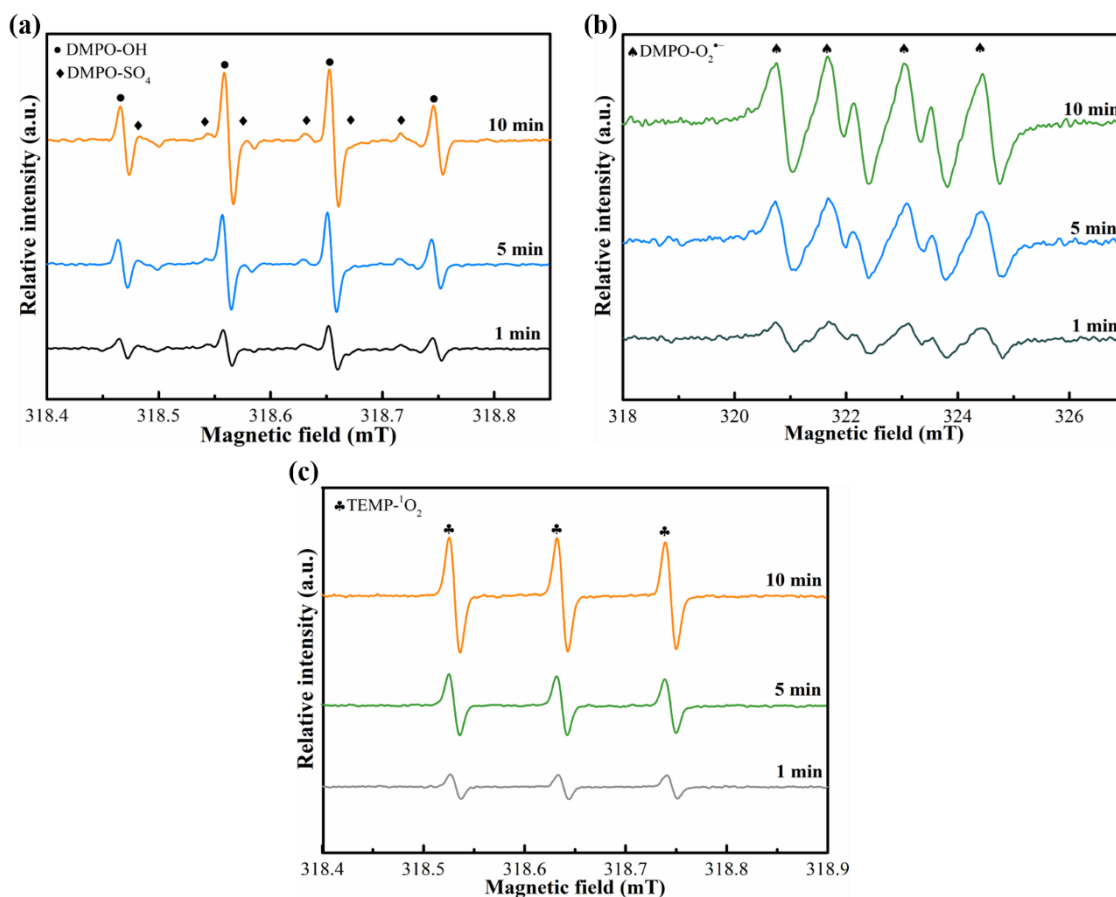


Fig. 1 Electron spin resonance analysis of BBC by using DMPO and TEMP as trapping agents in BBC/PS system ($O_2^{\cdot-}$ was detected in methanol circumstance). [ACT] = 20 mg/L, [PS] = 1 g/L, [BBC] = 0.1 g/L, [Temp] = 298 K.

Generally, persulfate activation system could degrade the pollutant by radical pathway and non-radical pathway. While the most common types of free radicals in PS activation system are $SO_4^{\cdot-}$, $\cdot OH$, $O_2^{\cdot-}$, the non-radical pathway is consisted by 1O_2 and electron transfer process [20]. To further explore the role of radical pathway and non-radical pathway, LSV and active species capture experiment were taken respectively (Fig. 2). According to previous studies, BQ and NaN_3 were chosen to explore the role of $O_2^{\cdot-}$ and 1O_2 , respectively [30, 38]. While EtOH is effective for both $SO_4^{\cdot-}$ and $\cdot OH$ ($k_{\cdot OH} = (1.2\text{--}2.8) \times 10^9 \text{ M}^{-1} \text{ s}^{-1}$, $k_{SO_4^{\cdot-}} = (1.6\text{--}7.8) \times 10^7 \text{ M}^{-1} \text{ s}^{-1}$), TBA can only capture $\cdot OH$

immediately ($k_{\cdot\text{OH}} = (3.8\text{--}7.6) \times 10^8 \text{ M}^{-1} \text{ s}^{-1}$, $k_{\text{SO}_4^{\cdot-}} = 4 \times 10^5 \text{ M}^{-1} \text{ s}^{-1}$). Consequently, when the EtOH and TBA are both selected as trapping agent, the role of $\text{SO}_4^{\cdot-}$ and $\cdot\text{OH}$ in PS activation system can be evaluated [29]. In this study, excess trapping agents were added in the BBC/PS system, and the variation of k_{obs} exhibited that each trapping agent could inhibit the catalytic process. After the addition of excess TBA, BQ, and NaN_3 , the k_{obs} reduced from 0.3111 min^{-1} to 0.2306 min^{-1} , 0.2403 min^{-1} and 0.2834 min^{-1} , respectively. The result verified the existence of $\cdot\text{OH}$, $\text{O}_2^{\cdot-}$ and $^1\text{O}_2$, and the greater variation of k_{obs} illustrated that $\cdot\text{OH}$ was more important in this system. Besides, the inhibition effect of EtOH (0.2196 min^{-1}) was stronger than that of TBA (Fig. 2a), which demonstrates the appearance of $\text{SO}_4^{\cdot-}$ in BBC/PS system. Extrapolating from the relatively small gap with the inhibitory effect of EtOH and TBA, the $\cdot\text{OH}$ might be the major radical in BBC/PS system. The active species quenching experiment unveiled that the $\text{SO}_4^{\cdot-}$, $\cdot\text{OH}$, $\text{O}_2^{\cdot-}$ and $^1\text{O}_2$ all worked in BBC/PS system (Eq. (3-5)). $\text{SO}_4^{\cdot-}$ might be produced by reaction with PS and H_2O , and the $\text{O}_2^{\cdot-}$ could be generated at the same time. Furthermore, free $\text{SO}_4^{\cdot-}$ in BBC/PS system could further generate $\cdot\text{OH}$.



However, none of the trapping agent can immediately terminate the degradation process, so, the non-radical pathway (electron transfer process) (Eq. (2)) might be the principal factor in this system. LSV was measured in 20 mM PBS to analyze the effect of

electron transfer process [39, 40]. The variation of current could assess the electron transfer capacity in the corresponding system. As showed in Fig. 2b, although PS and ACT were all added to the solution, there was almost no current response in bare glassy carbon electrode (GCE). After ornamenting by BBC, electron transfer ability was improved. Only when PS and ACT both existed, the current reached a peak. It supported the existence of electron transfer process in BBC/PS system. Aside from LSV, electron capture experiment also applied to verify the effect of electron transfer process in PS activation system. For probing into the proportion of electron transfer process in BBC/PS system, K_2CrO_4 was added [41]. The sharp decrement of k_{obs} (from 0.3111 min^{-1} to 0.065 min^{-1}) supported that the electron transfer process dominated the degradation of ACT. In conclusion, when ACT was chosen as the aim pollutant, both radical and non-radical pathway worked in the BBC/PS system and the non-radical pathway (electron transfer process) had a greater impact on ACT degradation.

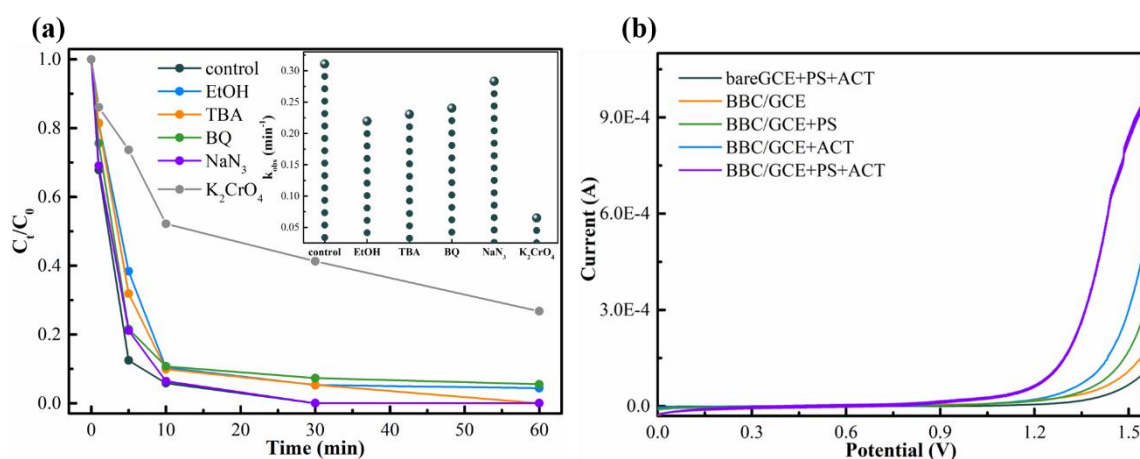


Fig. 2 (a) Effect of EtOH (0.75 M), TBA (0.75 M), BQ (1 mM), NaN_3 (1 mM), and K_2CrO_4 (1 mM) on ACT degradation in BBC/PS system and the insert presented corresponding pseudo-first-order rate constants, (b) LSV obtained by the bare GCE

electrode and BBC ornamented GCE electrode (BBC/GCE) in the presence of PS or ACT.

[ACT] = 20 mg/L, [PS] = 1 g/L, [BBC] = 0.1 g/L, [Temp] = 298 K.

3.2 The role of functional structure of BBC

Since biochar was applied in the PS activation system, various functional structures have been reported to be closely related to the catalytic capacity of biochar. Acid treatment and high temperature treatment are the common means to change the functional structure of carbon materials. Consequently, studies were launched to explore the specific role of these functional structures.

Swine bone is consisted by organic component (25 wt.%), inorganic component (65 wt.%), and water (10 wt.%) [42]. The main organic and inorganic components of bone are collagen and hydroxyapatite. While the collagens serve as the carbon source for BBC, the vast hydroxyapatite might block or cover the pore of carbon structure. For hydroxyapatite is intolerant to acidity, the acid treatment was applied to explore the effect of residual hydroxyapatite. The results showed that acid treatment is the critical step in BBC synthesis, because this process can boost the catalytic ability of BBC. For further understanding the relationship between functional structures and acid treatment, BBC-WA was involved. In addition, researches have reported that high-temperature treatment was a valid way to deactivate the oxygen-containing groups and generate defects on carbonaceous materials [43, 44]. So, the BBC was carbonized in 1300 °C (labeled as BBC-1300) and the resulting material was applied for further study. The effect of these treatments on BBC is directly reflected in the change of specific surface area. The acid treatment might wipe off the inorganic component on the biochar, which blocked the pore

in BBC-WA. Hence, the specific surface area boosted from 112 m²/g to 1024 m²/g after the acid treatment. The specific surface area of BBC-1300 climbed to 1157 m²/g, which illustrated that high temperature treatment could further increase the specific surface area.

XRD and Raman were taken to analyze the structural changes of BBC-WA and BBC-1300. In Fig. 3a, the peaks at (002) and (100) were attributed to the amorphous structure, and there is no obvious difference in crystal structure between BBC and BBC-1300. Besides, peaks around 32 ° and 40 ° indicated the existence of CaSi₂ and hydroxyapatite in BBC-WA (JCPDS Card No. 73-1964). The different between BBC and BBC-WA might contribute to the removal of inorganic component in swine bone, which might cover or block the carbon structure, ultimately, the peak of amorphous structure was hidden. This speculation could be supported by the soaring of specific surface area after acid treatment. With respect to Raman spectrum, generally, the peaks at 1580 cm⁻¹ and 1350 cm⁻¹ are the signal of graphite structure and defects, and the ratio of I_D and I_G represents the disorder degree of carbonaceous materials. The results of Raman spectrum illustrated that the high temperature treatment (1300 °C) endowed the BBC with more defects, which is in line with previous study [45].

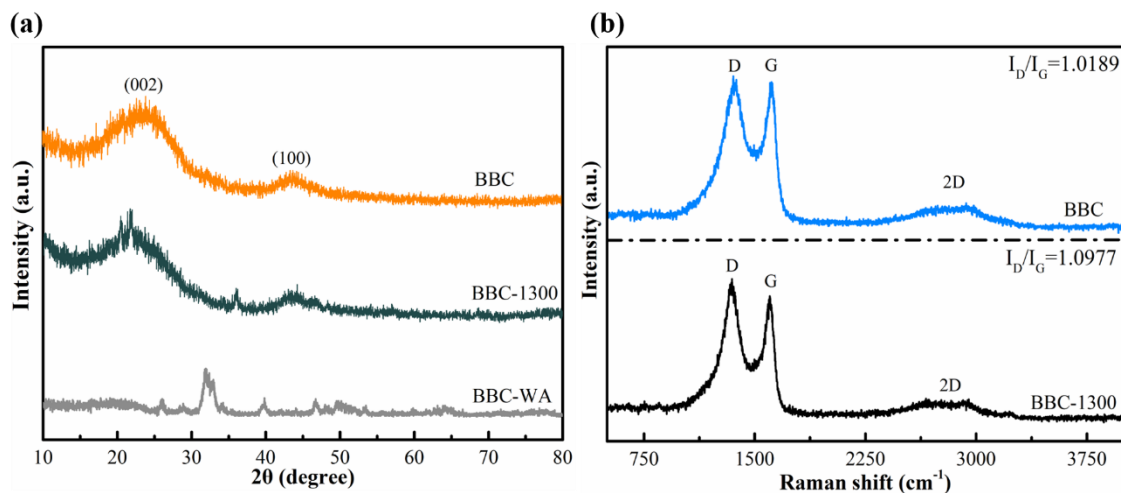


Fig. 3 (a) X-ray diffraction pattern of BBC, BBC-WA and BBC-1300, (b) the Raman spectra of BBC and BBC-1300.

FTIR (Fig. S2) and XPS were applied to explore the surface functional groups and elementary composition on these materials. FTIR spectra manifests that the BBC, BBC-WA and BBC-1300 all have ketone (C=O), hydroxyl (-OH) and carboxyl (-COOH). The FTIR spectra pattern of BBC was similar to that of BBC-1300, but the transmittance of each peak experienced a decrement after high temperature treatment. It proved that the high temperature might be able to deactivate all oxygen-containing groups on the BBC. The difference in the pattern and the transmittance between BBC and BBC-WA might result from the great distinction of elementary composition. Thus, the role XPS survey was taken to explore the variation of composition differences among BBC, BBC-WA and BBC-1300. On the whole, acid treatment and high temperature processing could reduce the oxygen content in the materials. The information given by Table 1 declared that the oxygen content of BBC-WA plummeted to 9.36% after acid processing, and the oxygen content of BBC-1300 was lower than that of BBC. Furthermore, the peaks of Ca2p, Na1s and P2p in the XPS survey spectra of BBC-WA could prove the retention of the natural inorganic component (hydroxyapatite). The vanishing of peaks of Ca2p, Na1s, P2p, etc. verified that the acid treatment removed the residual hydroxyapatite on BBC-WA, which was consistent with the result of XRD.

Table 1 Relative amount of carbon and oxygen in BBC, BBC-WA, and BBC-1300 (Atomic, %)

Samples	C	O
---------	---	---

BBC-WA	50.06%	49.94%
BBC	90.64%	9.36%
BBC-1300	94.81%	5.19%

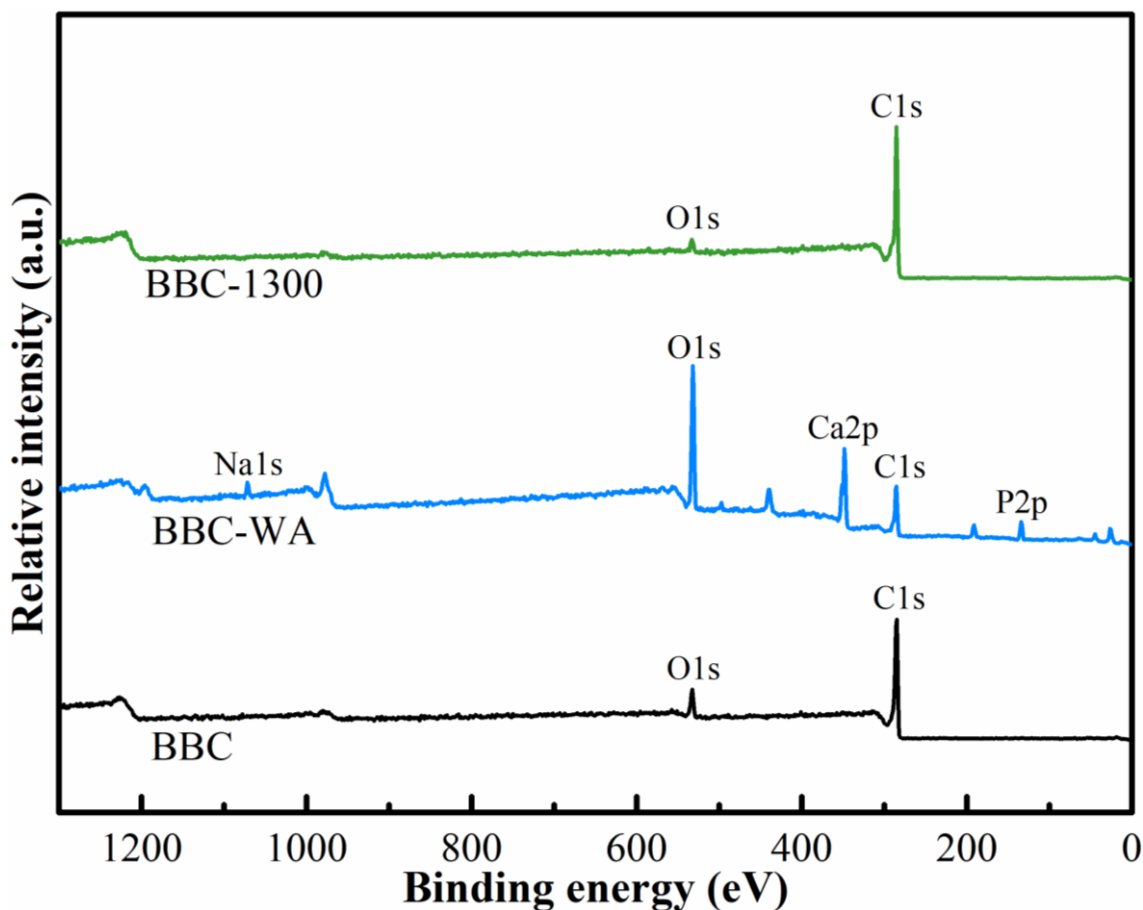


Fig. 4 XPS survey of BBC, BBC-WA and BBC-1300.

BBC-WA and BBC-1300 were applied in PS activation system to further explore the effect of structure on catalysis. Results showed that the adsorption capacity of BBC-1300 was higher than that of BBC, and almost no ACT was adsorbed on BBC-WA (Fig. S1). The catalytic efficiency of BBC-WA and BBC-1300 was lower than that of BBC. To be specific, the k_{obs} decreased to 0.2409 min^{-1} after high temperature processing, and the k_{obs} of BBC-WA was 0.1600 min^{-1} . **Active species** capture experiment (Fig. 5) and LSV (Fig.

S3) were taken to further understand the mechanism. Surprisingly, significant changes in degradation mechanisms could be observed. Unlike the BBC/PS system, which was dominated by electron transfer process, the role of electron transfer process in BBC-WA/PS and BBC-1300/PS system were obviously suppressed. While the effect of $^1\text{O}_2$ and $\text{O}_2^{\cdot-}$ were enlarged in BBC-WA/PS system, the role of $^1\text{O}_2$, $\text{O}_2^{\cdot-}$ and $\text{SO}_4^{\cdot-}$ were magnified in BBC-1300/PS system (The specific k_{obs} have presented in Table S2).

The low removal efficiency of BBC-WA/PS system might be due to the low adsorption capacity to ACT (Fig. S1). Generally, the adsorption of organic contaminants on biochar mainly relies on electrostatic interaction, hydrophobic effect, hydrogen bonds, and pore-filling. Oxygen-containing groups (such as -COOH and -OH) and the specific surface area were deemed as the key factor, which predominate the adsorption of organic contaminant on biochar [46]. However, the relatively high oxygen content in BBC-WA did not promote the adsorption of ACT, while the decrement of oxygen in BBC-1300 had no obvious adverse effect to its adsorption capacity. Additionally, comparing BBC, BBC-WA, and BBC-1300, the specific surface area and adsorption capacity is positively correlated. Hence, the specific surface area might be the major factor for the adsorption capacity.

Theoretically, both radical and non-radical pathway rely on the adsorption process. The BBC/WA maintained the degradation ability to ACT in some extent might owe to the collision caused by magnetic agitation. Thus, the electron transfer process, which is more dependent on the adsorption process, nearly played no role in BBC-WA/PS system. Although the specific surface area of BBC-1300 was higher than BBC and a stronger

adsorption capacity could be observed, the role of electron transfer process still suffered an abatement. It might be due to other structure changes caused by the high temperature treatment.

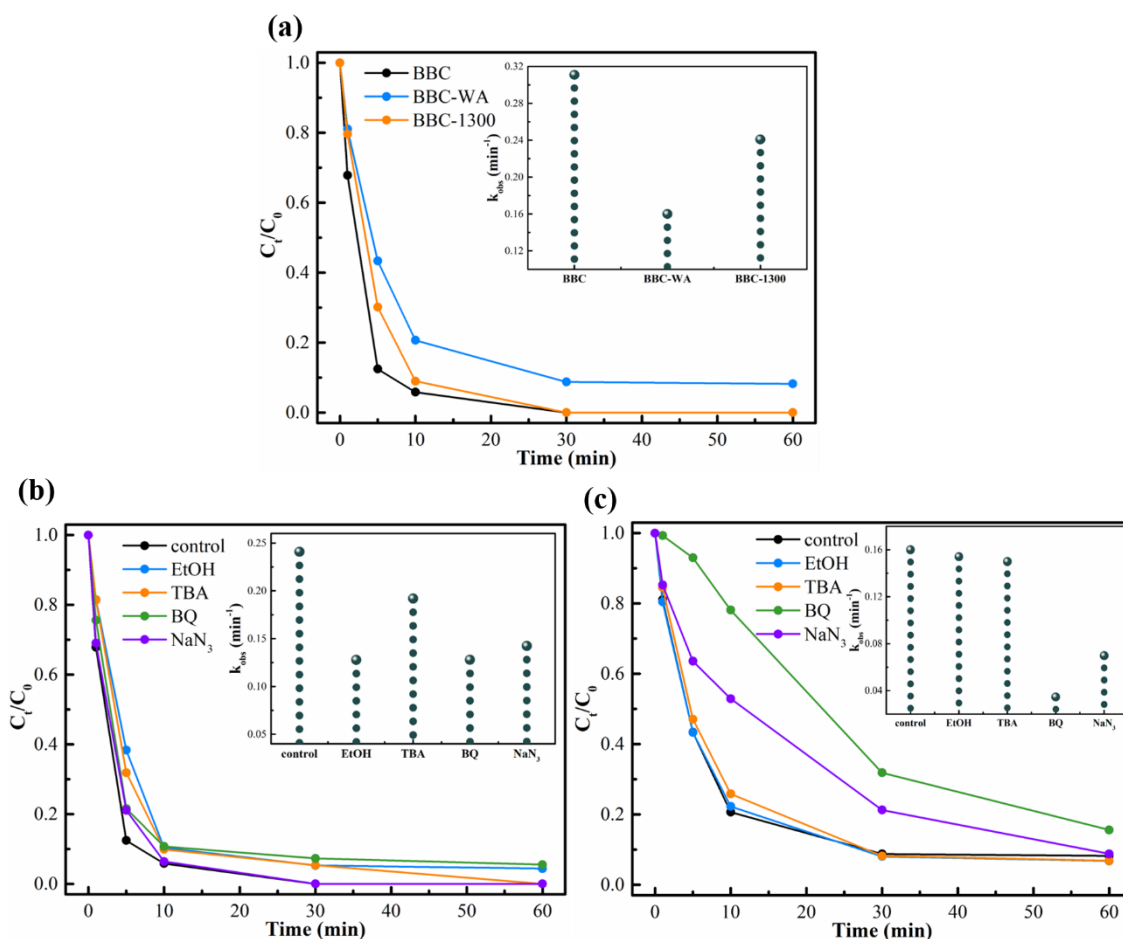


Fig. 5 (a) The catalytic performance of BBC, BBC-WA and BBC-1300, (b, c) **active species** capture experiment of BBC-1300 and BBC-WA respectively. The insert was the corresponding pseudo-first-order rate constants. $[ACT] = 20 \text{ mg/L}$, $[PS] = 1 \text{ g/L}$, $[BBC] = 0.1 \text{ g/L}$, $[EtOH] = 0.75 \text{ M}$, $[TBA] = 0.75 \text{ M}$, $[BQ] = 1 \text{ mM}$, $[NaN_3] = 1 \text{ mM}$, $[Temp] = 298 \text{ K}$.

Among various functional structures of biochar, oxygen-containing groups were commonly reported to serve as active sites. For investigating the role of different oxygen-containing functional groups in BBC/PS system, the selective inactivation experiments

of functional groups were conducted. As mentioned above, previous studies had applied organic reagents to selectively deactivate the oxygen-containing functional groups on carbon materials [31, 32]. Specifically, the PH, BA and BrPE could selectively react with -C=O, -OH and -COOH on carbonaceous material without affecting other groups (Scheme 1). Absolutely, this method was proved to have little effect on other characteristic structure of the target materials. Besides, in the modification process, BBC would be soaked and stirred in an organic solvent. In order to avoid the influence of the organic solvent, BBC was soaked and stirred in organic solvent without inactivator, which was labeled as BBC-EA.

XPS survey and O1s (Fig. 6) high resolution spectrum were taken to verify the success of selective inactivation of modified BBC (Fig. 6). According to O1s high resolution spectrums, peaks around 522.5 eV and 523.6 eV represented the vibrations of C-OH/C-O-C and C=O, respectively. Abatement in the content of C=O and -OH could be directly observed, after embellishing by PH and BA, respectively. While the BBC and BBC-BrPE have a similar proportion of C=O and -OH, the climbing of Zeta potential (pH=7) after BrPE decoration proved the inactivation of COOH in BBC (Fig. S4).

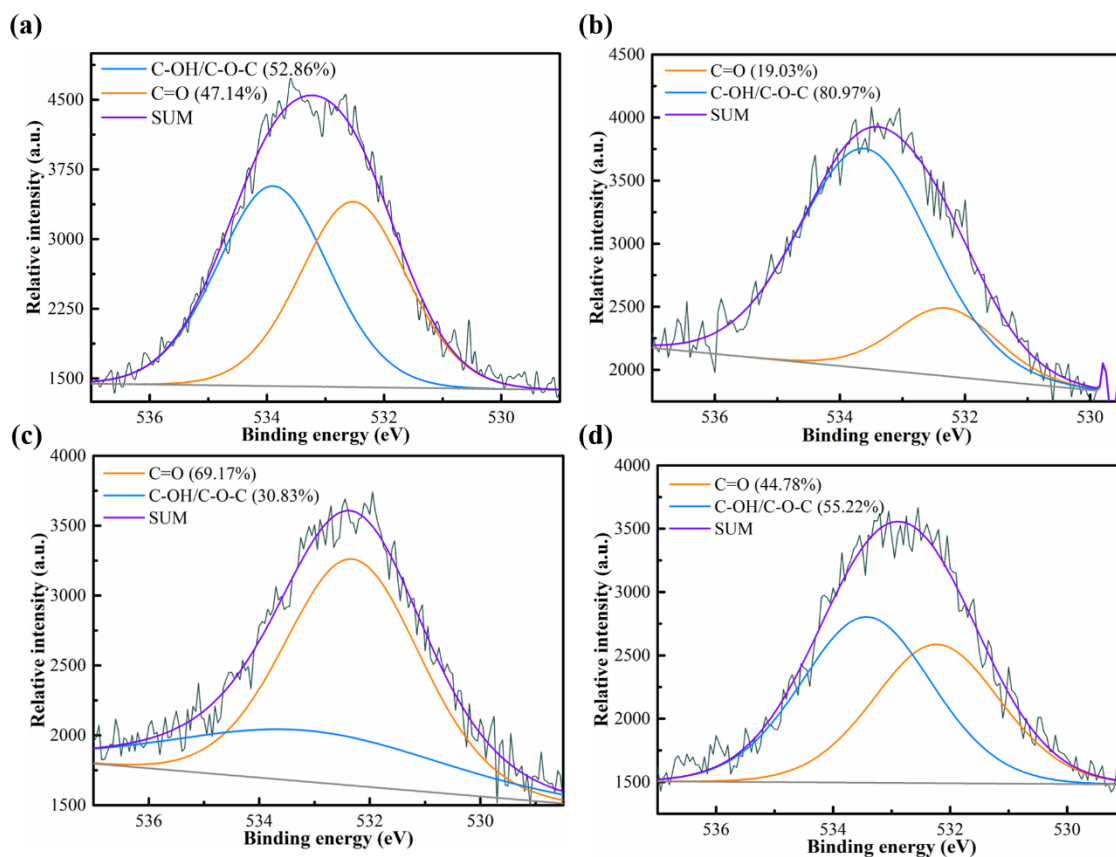


Fig. 6 O1s spectrums of (a) BBC, (b) BBC-PH, (c) BBC-BA and (d) BBC-BrPE.

As shown in Fig. 7a, the soak and stir process accelerated the catalysis, for it might diminish the particle size so that the BBC-EA was more evenly dispersed in the water. Although the decline of k_{obs} could be observed after modified by PH, BA, and BrPE, the PH showed the strongest inhibitory effect. Specifically, the k_{obs} of BBC-PH attenuated to 0.1816 min^{-1} . While the PH, BA, and BrPE were aimed at C=O, -OH, and -COOH, respectively, the selective inactivation experiments manifested that C=O, -OH, and -COOH all work in BBC/PS system, and the C=O was the most powerful one. It was in accordance with previous studies that C=O acts as the active site in PS activation system [25, 47]. With respect to active species in BBC/PS system, $\text{SO}_4^{\cdot-}$, $\cdot\text{OH}$, $\text{O}_2^{\cdot-}$ and $^1\text{O}_2$ were all contributed to PS activation system, when BBC-PH, BBC-BA and BBC-BrPE served as catalyst. Albeit the proportion of different species active species in BBC-BrPE/PS and

BBC-BA/PS system is similar to that of BBC/PS system (the role of $\cdot\text{OH}$ and $\text{SO}_4^{\cdot-} > \text{O}_2^{\cdot-} > {}^1\text{O}_2$), the inhibitory effects of trapping agent were slightly declined (The specific k_{obs} have presented in Table S2). Thus, the -COOH and -OH might be the active sites for generating radicals, the conclusion is consistent with the previous studies that the -COOH and -OH on biochar could promote the production of radicals [27, 48]. Comparing to BBC/PS and BBC-BrPE/PS system, the gap between the inhibition of EtOH and TBA was larger in BBC-BA/PS system. In brief, the role of $\text{SO}_4^{\cdot-}$ was highlighted after the inactivation of -OH. Under this fact, -OH might be able to act as the active sites to produce $\cdot\text{OH}$. Besides, the effect of $\cdot\text{OH}$ was inhibited when C=O was deactivated. It might be a reasonable deduction that in BBC/PS system C=O could be the active sites to produce $\cdot\text{OH}$.

LSV were also taken to investigate the **electron transfer process**. LSV obtained by BBC-BA and **BBC-BrPE** ornamented GCE electrode in the presence of both PS and ACT were roughly the same as that of BBC. Conversely, a visible decline of LSV current could be seen when GCE was ornamented by BBC-PH. **It was a strong evidence to prove the C=O was the active sites for electron transfer pathway (Fig. S3).**

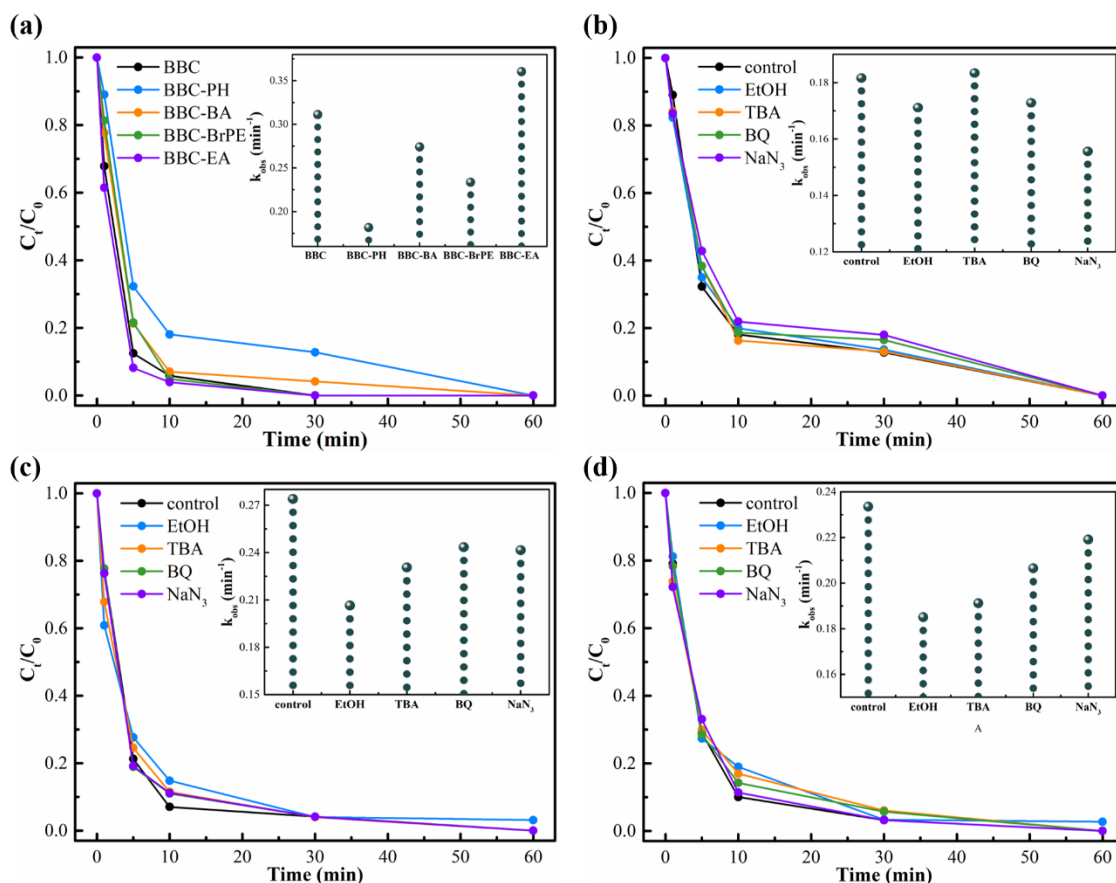


Fig. 7 (a) The catalytic performance of BBC, BBC-PH, BBC-BA, BBC-BrPE and BBC-EA, active species capture experiment of (b) BBC-PH, (c) BBC-BA and (d) BBC-BrPE respectively. The insert was the corresponding pseudo-first-order rate constants. $[ACT] = 20$ mg/L, $[PS] = 1$ g/L, $[BBC] = 0.1$ g/L, $[EtOH] = 0.75$ M, $[TBA] = 0.75$ M, $[BQ] = 1$ mM, $[NaN_3] = 1$ mM, $[Temp] = 298$ K.

Taken all BBC and its derivatives into account, the concrete relationship between functional structures and mechanisms became clear (Table 2). The roles of $O_2^{\cdot-}$ and 1O_2 were magnified in BBC-WA/PS system. In consideration of oxygen-containing groups are always reported as the active sites in PS activation system, the different proportion of different species of active species might account for the different content and type of oxygen-containing groups. According to the selective inactivation experiment, none of

the oxygen-containing groups could help to generate $O_2^{\cdot-}$ and 1O_2 . Thus, the difference between BBC and BBC-WA might be embodied in the existence of inorganic component in BBC-WA. In view of the structure difference between these materials, it was reasonable to infer that the hydroxyapatite remained in BBC-WA could stimulate production of $O_2^{\cdot-}$. Furthermore, on the basis of the reaction mechanism, excess $O_2^{\cdot-}$ could react with $\cdot OH$ or H^+ to produce 1O_2 (Eq. (6-7)).



BBC-1300 deactivated all kinds of oxygen-containing groups and obtained more defects. The selective inactivation experiment proved that C=O was the active sites for electron transfer process, so that the little minor role of electron transfer process might result from the inactivation of C=O. However, the catalytic efficiency of BBC-1300 (0.2409 min^{-1}) was higher than BBC-PH (0.1816 min^{-1}), albeit the LSV current of BBC-1300 was lower than BBC-PH. This might be due to other structural changes brought by high temperature treatment. It was obviously that the inhibition of BQ and NaN_3 (trapping agent of $O_2^{\cdot-}$ and 1O_2) are more potent than that of BBC/PS system. On the basis of previous study, the enlargement of the role of $O_2^{\cdot-}$ and 1O_2 might owe to the increase of defects [33]. The greater gap between the inhibition of EtOH and TBA demonstrated that the proportion of $SO_4^{\cdot-}$ was amplified after high temperature treatment. Based on the results of selective inactivation experiment, the increase in the role of $SO_4^{\cdot-}$ might because of the abatement of -OH on BBC-1300.

Table 2 The concrete relationship between functional structures and mechanisms.

Active sites	Mechanisms
-OH, -COOH	$\text{SO}_4^{\cdot-}$, $\cdot\text{OH}$
Defects and inorganic component	$\text{O}_2^{\cdot-}$, $^1\text{O}_2$
-C=O	$\cdot\text{OH}$, Electron transfer process

3.3 The effect of water matrices and stability tests

As a typical kind of PPCPs, ACT does not generally appear alone in wastewater. Studies have proved that inorganic anions (such as Cl^- , NO_3^-) and natural organic matters (NOMs) might influence the catalytic performance of PS activation system [49]. They could serve as the capture agents of radicals in PS activation system, ultimately diminish degradation efficiency for ACT. Hence, experiments were taken to confirm the influence of water matrices to BBC/PS system.

Fig. 8a manifested that both Cl^- and NO_3^- could slightly impair the degradation capacity of BBC/PS system, while humic acid (HA) could promote this process. According to previous studies, the inorganic anions primarily work through trapping the radicals [18, 28]. The results showed that Cl^- and NO_3^- had little effect on the degradation process, it supported the deduction that ACT was mainly degrade by non-radical pathway. It has been reported that the Cl^- acts on both non-radical and radical pathway. Specifically, Cl^- could restrain the degradation process by capturing the radical (Eq. (8)-(11)), and excess Cl^- in aqueous media could accelerate the electron transfer in non-radical pathway [28, 50]. For further understanding, experiments were conducted the effect of different concentrations of Cl^- (Fig. S5). While 5 mM Cl^- was added, an inhibition could be

observed. With the climbing of Cl^- concentration, there was a decrease of inhibition. An improvement of degradation efficiency could be seen when the concentration of Cl^- reach 20 mM. This phenomenon was in line with the previous studies [19, 51]. HA was chosen as the typical NOMs to explore the effect of NOMs on BBC/PS system. Unlike some published reports, the HA shows a pronounced positive impact on ACT degradation. It may be owe to the sole phenol, semi-quinone groups and quinone molecules in NOMs, which could generate $\text{SO}_4^{\cdot-}$ and $\cdot\text{OH}$ by activating PS [52, 53].

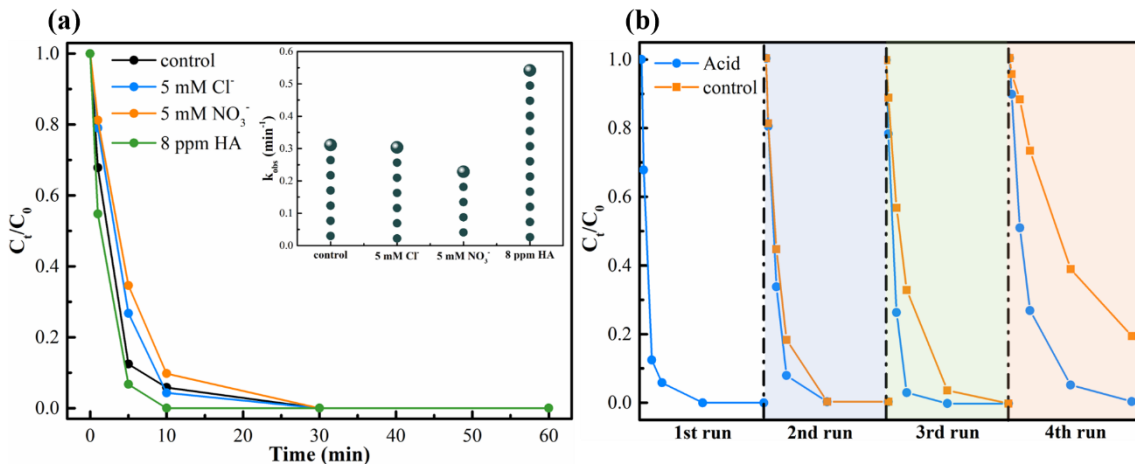


Fig. 8 (a) Effect of the given concentration Cl^- , NO_3^- and HA, the insert presented corresponding pseudo-first-order rate constants, (b) The stability test of BBC/PS system [ACT] = 20 mg/L, [PS] = 1 g/L, [BBC] = 0.1 g/L, [Temp] = 298 K.

Stability experiment is an alternative option to investigate the promising application of BBC. Fig. 8b showed the stability test of BBC with and without acid treatment. An

obvious decline of degradation rate for the recycled BBC without acid treatment could be seen. However, the k_{obs} of recycled BBC with acid treatment could maintain at 0.2371 min^{-1} after 4th run (Fig. S6). It illuminated that the acid treatment was an effective way to enhance the stability of BBC.

4. Conclusion

To sum up, BBC could be applied in PS activation system to degrade ACT effectively, and both radical and non-radical pathway were worked in this system. Water matrices had little effect on BBC/PS system, and the BBC possessed an excellent stability. However, non-radical pathway (electron transfer process) dominated the degradation process. Among various worked radical species, $\cdot\text{OH}$ might have the greatest impact on this system. Different from traditional research methods, selective inactivation of oxygen-containing groups was applied to investigate the active sites of BBC. Combining with the experimental results of BBC-WA and BBC-1300, these corollaries were presented: (a) electron transfer process was highly contingent on C=O; (b) residual hydroxyapatite and defects might stimulate PS to produce $\text{O}_2^{\cdot-}$ and $^1\text{O}_2$; (c) -OH and -COOH were the active sites for radical pathway; (d) C=O might be the active sites to produce $\cdot\text{OH}$ in BBC/PS system. In general, each of $\text{SO}_4^{\cdot-}$, $\cdot\text{OH}$, $\text{O}_2^{\cdot-}$, $^1\text{O}_2$ and electron transfer process had its own advantages in different environments. Since biochar was used in catalysis field, various characteristic structures were reported to work in PS activation system. Whereas the specific role of structures has not been studied. Understanding the mechanism of different characteristic structures is helpful to the oriented synthesis of biochar in practical application. This study gives a brand-new perspective to application of biochar in catalysis.

Acknowledgements

This study was financially supported by the Program for the National Natural Science Foundation of China (51521006, 51879101, 51579098, 51779090, 51709101, 51809090, 51278176, 51378190), the National Program for Support of Top-Notch Young Professionals of China (2014), the Program for Changjiang Scholars and Innovative Research Team in University (IRT-13R17), and Hunan Provincial Science and Technology Plan Project (2018SK20410, 2017SK2243, 2016RS3026), and the Fundamental Research Funds for the Central Universities (531118010473, 531119200086, 531118010114, 531107050978), The Three Gorges Follow-up Research Project (2017HXXY-05).

Reference

- [1] D. Jiang, M. Chen, H. Wang, G. Zeng, D. Huang, M. Cheng, Y. Liu, W. Xue, Z. Wang, The application of different typological and structural MOFs-based materials for the dyes adsorption, *Coordination Chemistry Reviews* 380 (2019) 471-483.
- [2] L. Qin, H. Yi, G. Zeng, C. Lai, D. Huang, P. Xu, Y. Fu, J. He, B. Li, C. Zhang, Hierarchical porous carbon material restricted Au catalyst for highly catalytic reduction of nitroaromatics, *Journal of hazardous materials* 380 (2019) 120864.
- [3] H. Yi, M. Li, X. Huo, G. Zeng, C. Lai, D. Huang, Z. An, L. Qin, X. Liu, B. Li, Recent development of advanced biotechnology for wastewater treatment, *Critical reviews in biotechnology* 40 (2020) 99-118.
- [4] W. Wang, Q. Niu, G. Zeng, C. Zhang, D. Huang, B. Shao, C. Zhou, Y. Yang, Y. Liu, H. Guo, 1D porous tubular g-C₃N₄ capture black phosphorus quantum dots as 1D/0D metal-free photocatalysts for oxytetracycline hydrochloride degradation and hexavalent chromium reduction, *Applied Catalysis B: Environmental* (2020) 119051.
- [5] B. Li, C. Lai, G. Zeng, D. Huang, L. Qin, M. Zhang, M. Cheng, X. Liu, H. Yi, C. Zhou, Black Phosphorus, a Rising Star 2D Nanomaterial in the Post-Graphene Era: Synthesis, Properties, Modifications, and Photocatalysis Applications, *Small* 15 (2019) 1804565.
- [6] B. Li, C. Lai, G. Zeng, L. Qin, H. Yi, D. Huang, C. Zhou, X. Liu, M. Cheng, P. Xu, Facile hydrothermal synthesis of Z-scheme Bi₂Fe₄O₉/Bi₂WO₆ heterojunction photocatalyst with enhanced visible light photocatalytic activity, *ACS applied materials & interfaces* 10 (2018) 18824-18836.
- [7] L. Qin, Z. Zeng, G. Zeng, C. Lai, A. Duan, R. Xiao, D. Huang, Y. Fu, H. Yi, B. Li, Cooperative catalytic performance of bimetallic Ni-Au nanocatalyst for highly efficient hydrogenation of nitroaromatics and corresponding mechanism insight, *Applied Catalysis B: Environmental* 259 (2019) 118035.
- [8] X. Zhou, C. Lai, D. Huang, G. Zeng, L. Chen, L. Qin, P. Xu, M. Cheng, C. Huang, C. Zhang, Preparation of water-compatible molecularly imprinted thiol-functionalized activated titanium dioxide: Selective adsorption and efficient photodegradation of 2, 4-dinitrophenol in aqueous solution, *Journal of hazardous materials* 346 (2018) 113-123.
- [9] H. Yi, M. Yan, D. Huang, G. Zeng, C. Lai, M. Li, X. Huo, L. Qin, S. Liu, X. Liu, Synergistic effect

of artificial enzyme and 2D nano-structured Bi₂WO₆ for eco-friendly and efficient biomimetic photocatalysis, *Applied Catalysis B: Environmental* (2019).

[10] C. Lai, M. Zhang, B. Li, D. Huang, G. Zeng, L. Qin, X. Liu, H. Yi, M. Cheng, L. Li, Fabrication of CuS/BiVO₄ (0 4 0) binary heterojunction photocatalysts with enhanced photocatalytic activity for Ciprofloxacin degradation and mechanism insight, *Chemical Engineering Journal* 358 (2019) 891-902.

[11] Y. Fu, L. Qin, D. Huang, G. Zeng, C. Lai, B. Li, J. He, H. Yi, M. Zhang, M. Cheng, Chitosan functionalized activated coke for Au nanoparticles anchoring: Green synthesis and catalytic activities in hydrogenation of nitrophenols and azo dyes, *Applied Catalysis B: Environmental* 255 (2019) 117740.

[12] Y. Yang, C. Zhang, C. Lai, G. Zeng, D. Huang, M. Cheng, J. Wang, F. Chen, C. Zhou, W. Xiong, BiOX (X = Cl, Br, I) photocatalytic nanomaterials: Applications for fuels and environmental management, *Advances in Colloid and Interface Science* 254 (2018).

[13] C. Zhou, Z. Zeng, G. Zeng, D. Huang, R. Xiao, M. Cheng, C. Zhang, W. Xiong, C. Lai, Y. Yang, Visible-light-driven photocatalytic degradation of sulfamethazine by surface engineering of carbon nitride: Properties, degradation pathway and mechanisms, *Journal of hazardous materials* 380 (2019) 120815.

[14] B. Song, Z. Zeng, G. Zeng, J. Gong, R. Xiao, S. Ye, M. Chen, C. Lai, P. Xu, X. Tang, Powerful combination of g-C₃N₄ and LDHs for enhanced photocatalytic performance: A review of strategy, synthesis, and applications, *Advances in colloid and interface science* (2019) 101999.

[15] Y. Zhang, X. Yuan, W. Lu, Y. Yan, J. Zhu, T.-W. Chou, MnO₂ based sandwich structure electrode for supercapacitor with large voltage window and high mass loading, *Chemical Engineering Journal* 368 (2019) 525-532.

[16] C. Lai, F. Huang, G. Zeng, D. Huang, L. Qin, M. Cheng, C. Zhang, B. Li, H. Yi, S. Liu, L. Li, L. Chen, Fabrication of novel magnetic MnFe₂O₄/bio-char composite and heterogeneous photo-Fenton degradation of tetracycline in near neutral pH, *Chemosphere* 224 (2019) 910-921.

[17] A.V. Levanov, O.Y. Isaikina, R.B. Gasanova, A.S. Uzhel, V.V. Lunin, Kinetics of chlorate formation during ozonation of aqueous chloride solutions, *Chemosphere* 229 (2019) 68-76.

[18] T. Zhang, Y. Chen, Y. Wang, J. Le Roux, Y. Yang, J.-P. Crou é Efficient Peroxydisulfate Activation Process Not Relying on Sulfate Radical Generation for Water Pollutant Degradation, *Environmental*

Science & Technology 48 (2014) 5868-5875.

[19] L. Tang, Y. Liu, J. Wang, G. Zeng, Y. Deng, H. Dong, H. Feng, J. Wang, B. Peng, Enhanced activation process of persulfate by mesoporous carbon for degradation of aqueous organic pollutants: Electron transfer mechanism, *Applied Catalysis B: Environmental* 231 (2018) 1-10.

[20] X. Duan, H. Sun, Z. Shao, S. Wang, Nonradical reactions in environmental remediation processes: Uncertainty and challenges, *Applied Catalysis B: Environmental* 224 (2018) 973-982.

[21] B. Song, M. Chen, S. Ye, P. Xu, G. Zeng, J. Gong, J. Li, P. Zhang, W. Cao, Effects of multi-walled carbon nanotubes on metabolic function of the microbial community in riverine sediment contaminated with phenanthrene, *Carbon* 144 (2019) 1-7.

[22] S. Ye, G. Zeng, H. Wu, C. Zhang, J. Dai, J. Liang, J. Yu, X. Ren, H. Yi, M. Cheng, Biological technologies for the remediation of co-contaminated soil, *Critical reviews in biotechnology* 37 (2017) 1062-1076.

[23] J.J. Manyà, Pyrolysis for biochar purposes: a review to establish current knowledge gaps and research needs, *Environmental science & technology* 46 (2012) 7939-7954.

[24] R.-Z. Wang, D.-L. Huang, Y.-G. Liu, C. Zhang, C. Lai, X. Wang, G.-M. Zeng, X.-M. Gong, A. Duan, Q. Zhang, Recent advances in biochar-based catalysts: properties, applications and mechanisms for pollution remediation, *Chemical Engineering Journal* (2019).

[25] B.-C. Huang, J. Jiang, G.-X. Huang, H.-Q. Yu, Sludge biochar-based catalysts for improved pollutant degradation by activating peroxydisulfate, *Journal of Materials Chemistry A* 6 (2018) 8978-8985.

[26] G. Fang, J. Gao, C. Liu, D.D. Dionysiou, Y. Wang, D. Zhou, Key role of persistent free radicals in hydrogen peroxide activation by biochar: implications to organic contaminant degradation, *Environmental science & technology* 48 (2014) 1902-1910.

[27] Y. Wu, J. Guo, Y. Han, J. Zhu, L. Zhou, Y. Lan, Insights into the mechanism of persulfate activated by rice straw biochar for the degradation of aniline, *Chemosphere* 200 (2018) 373-379.

[28] X.G. Duan, Z.M. Ao, L. Zhou, H.Q. Sun, G.X. Wang, S.B. Wang, Occurrence of radical and nonradical pathways from carbocatalysts for aqueous and nonaqueous catalytic oxidation, *Applied Catalysis B-Environmental* 188 (2016) 98-105.

[29] X. Zhou, Z. Zeng, G. Zeng, C. Lai, R. Xiao, S. Liu, D. Huang, L. Qin, X. Liu, B. Li, H. Yi, Y. Fu,

- L. Li, Z. Wang, Persulfate activation by swine bone char-derived hierarchical porous carbon: multiple mechanism system for organic pollutant degradation in aqueous, *Chemical Engineering Journal* (2019) 123091.
- [30] S. Liu, C. Lai, B. Li, C. Zhang, M. Zhang, D. Huang, L. Qin, H. Yi, X. Liu, F. Huang, X. Zhou, L. Chen, Role of radical and non-radical pathway in activating persulfate for degradation of p-nitrophenol by sulfur-doped ordered mesoporous carbon, *Chemical Engineering Journal* (2019) 123304.
- [31] W. Qi, W. Liu, B. Zhang, X. Gu, X. Guo, D. Su, Oxidative dehydrogenation on nanocarbon: identification and quantification of active sites by chemical titration, *Angewandte Chemie International Edition* 52 (2013) 14224-14228.
- [32] H. Sun, A. Zhao, N. Gao, K. Li, J. Ren, X. Qu, Deciphering a nanocarbon-based artificial peroxidase: chemical identification of the catalytically active and substrate-binding sites on graphene quantum dots, *Angewandte Chemie International Edition* 54 (2015) 7176-7180.
- [33] X. Cheng, H. Guo, Y. Zhang, G.V. Korshin, B. Yang, Insights into the mechanism of nonradical reactions of persulfate activated by carbon nanotubes: Activation performance and structure-function relationship, *Water Res* 157 (2019) 406-414.
- [34] M. Shen, Y. Zhang, Y. Zhu, B. Song, G. Zeng, D. Hu, X. Wen, X. Ren, Recent advances in toxicological research of nanoplastics in the environment: A review, *Environmental pollution* (2019).
- [35] X. Du, X. Bai, L. Xu, L. Yang, P. Jin, Visible-light activation of persulfate by TiO₂/g-C₃N₄ photocatalyst toward efficient degradation of micropollutants, *Chemical Engineering Journal* 384 (2020) 123245.
- [36] H.N.P. Vo, G.K. Le, T.M.H. Nguyen, X.-T. Bui, K.H. Nguyen, E.R. Rene, T.D.H. Vo, N.-D.T. Cao, R. Mohan, Acetaminophen micropollutant: Historical and current occurrences, toxicity, removal strategies and transformation pathways in different environments, *Chemosphere* 236 (2019) 124391.
- [37] W. Ren, L. Xiong, X. Yuan, Z. Yu, H. Zhang, X. Duan, S. Wang, Activation of Peroxydisulfate on Carbon Nanotubes: Electron-Transfer Mechanism, *Environmental Science & Technology* 53 (2019) 14595-14603.
- [38] L. Li, C. Lai, F. Huang, M. Cheng, G. Zeng, D. Huang, B. Li, S. Liu, M. Zhang, L. Qin, M. Li, J. He, Y. Zhang, L. Chen, Degradation of naphthalene with magnetic bio-char activate hydrogen peroxide:

Synergism of bio-char and Fe–Mn binary oxides, *Water Research* 160 (2019) 238-248.

[39] C. Lai, S. Liu, C. Zhang, G. Zeng, D. Huang, L. Qin, X. Liu, H. Yi, R. Wang, F. Huang, B. Li, T. Hu, Electrochemical Aptasensor Based on Sulfur–Nitrogen Codoped Ordered Mesoporous Carbon and Thymine–Hg²⁺–Thymine Mismatch Structure for Hg²⁺ Detection, *ACS Sensors* 3 (2018) 2566-2573.

[40] X. Liu, D. Huang, C. Lai, G. Zeng, L. Qin, H. Wang, H. Yi, B. Li, S. Liu, M. Zhang, Recent advances in covalent organic frameworks (COFs) as a smart sensing material, *Chemical Society Reviews* (2019).

[41] J. Yu, L. Tang, Y. Pang, G. Zeng, H. Feng, J. Zou, J. Wang, C. Feng, X. Zhu, X. Ouyang, J. Tan, Hierarchical porous biochar from shrimp shell for persulfate activation: A two-electron transfer path and key impact factors, *Applied Catalysis B: Environmental* 260 (2020).

[42] M.J. Olszta, X. Cheng, S.S. Jee, R. Kumar, Y.-Y. Kim, M.J. Kaufman, E.P. Douglas, L.B. Gower, Bone structure and formation: A new perspective, *Materials Science and Engineering: R: Reports* 58 (2007) 77-116.

[43] P.G. Collins, Defects and disorder in carbon nanotubes, *Oxford Handbook of Nanoscience and Technology Volume 2: Materials: Structures, Properties and Characterization Techniques*, Oxford University Press Oxford 2009, pp. 156-184.

[44] M.S. Dresselhaus, A. Jorio, M. Hofmann, G. Dresselhaus, R. Saito, Perspectives on carbon nanotubes and graphene Raman spectroscopy, *Nano letters* 10 (2010) 751-758.

[45] R. Andrews, D. Jacques, D. Qian, E.C. Dickey, Purification and structural annealing of multiwalled carbon nanotubes at graphitization temperatures, *Carbon* 39 (2001) 1681-1687.

[46] X. Tan, Y. Liu, G. Zeng, X. Wang, X. Hu, Y. Gu, Z. Yang, Application of biochar for the removal of pollutants from aqueous solutions, *Chemosphere* 125 (2015) 70-85.

[47] X. Duan, H. Sun, J. Kang, Y. Wang, S. Indrawirawan, S. Wang, Insights into Heterogeneous Catalysis of Persulfate Activation on Dimensional-Structured Nanocarbons, *ACS Catalysis* 5 (2015) 4629-4636.

[48] K.M. Zhu, X.S. Wang, D. Chen, W. Ren, H. Lin, H. Zhang, Wood-based biochar as an excellent activator of peroxydisulfate for Acid Orange 7 decolorization, *Chemosphere* 231 (2019) 32-40.

[49] X. Tang, G. Zeng, C. Fan, M. Zhou, L. Tang, J. Zhu, J. Wan, D. Huang, M. Chen, P. Xu,

Chromosomal expression of CadR on *Pseudomonas aeruginosa* for the removal of Cd (II) from aqueous solutions, *Science of the Total Environment* 636 (2018) 1355-1361.

[50] Z. Wang, R. Yuan, Y. Guo, L. Xu, J. Liu, Effects of chloride ions on bleaching of azo dyes by Co²⁺/oxone reagent: Kinetic analysis, *Journal of Hazardous Materials* 190 (2011) 1083-1087.

[51] C.T. Guan, J. Jiang, C.W. Luo, S.Y. Pang, Y. Yang, Z. Wang, J. Ma, J. Yu, X. Zhao, Oxidation of bromophenols by carbon nanotube activated peroxymonosulfate (PMS) and formation of brominated products: Comparison to peroxydisulfate (PDS), *Chemical Engineering Journal* 337 (2018) 40-50.

[52] M. Ahmad, A.L. Teel, R.J. Watts, Mechanism of Persulfate Activation by Phenols, *Environmental Science & Technology* 47 (2013) 5864-5871.

[53] G. Fang, J. Gao, D.D. Dionysiou, C. Liu, D. Zhou, Activation of Persulfate by Quinones: Free Radical Reactions and Implication for the Degradation of PCBs, *Environmental Science & Technology* 47 (2013) 4605-4611.